Future Nuclear and Hadronic Physics at the CERN-AD

Ab initio description of antiproton-deuteron hydrogenic states

Pierre-Yves Duerinck[1,2]

Collaborators: Jérémy Dohet-Eraly[1], Rimantas Lazauskas[2], and Jaume Carbonell[3]

[1]Physique nucléaire et physique quantique (PNPQ), ULB, Brussels
[2]Institut Pluridisciplinaire Hubert Curien (IPHC), Unistra, Strasbourg
[3]Université Paris-Saclay, CNRS/IN2P3, IJCLab, Orsay

April 08, 2024

Outline

Outline

1. Introduction
2. The $N\bar{N}$ interaction
3. Formalism
4. Results
5. Conclusion

Antiproton physics at CERN

- The interest for low-energy antiproton physics has been revived with the development of dedicated facilities at CERN: LEAR (1983-1996), AD, ELENA.
- Opportunity to study the properties of antimatter, exotic particle-antiparticle systems, and standard matter.
- PUMA project[1]: aims to study nucleus skin densities of short-lived nuclear isotopes produced by ISOLDE, using low-energy antiprotons transported from ELENA.

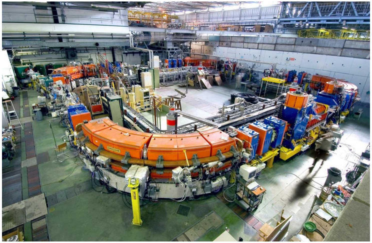

Figure: LEAR (Low Energy Antiproton Ring). Credits: CERN

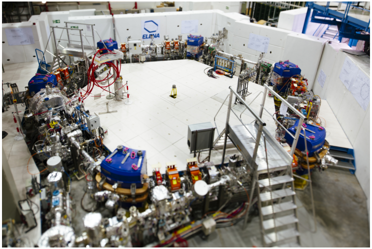

Figure: ELENA (Extra-Low Energy Antiproton Ring). Credits: CERN

[1] T. Aumann, A. Obertelli, *et al.* *Eur. J. Phys. A* **58** (2022) 88

AntiProton Unstable Matter Annihilation (PUMA) project

- The antiproton-nucleus annihilation is expected to happen in the periphery of the nucleus $\longrightarrow$ study of the nuclear density tail by measuring the $p\bar{p}/n\bar{p}$ annihilation ratio.
- A fully microscopic treatment of antiproton-nucleus systems remains to be developed.

- Remaining questions:
  1. How can we interpret the data from theoretical predictions ?
  2. Validity of the $N\bar{N}$ models ?
  3. Model dependence ?

$\longrightarrow$ Microscopic treatment of the antiproton-nucleus system.

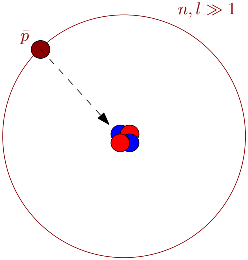

Figure: Antiproton-nucleus system

Antiproton-nucleus system

- Antiproton-nucleus system:
  1. Capture of the antiproton on a highly excited Coulomb orbital and formation of a quasi-bound state with

$$E = E_R - i\frac{\Gamma}{2}, \qquad E_R \approx E_B - \frac{\mathrm{Ryd}(\bar{\mathrm{p}}\mathrm{A})}{n^2}$$

  2. X-ray cascade and annihilation with a nucleon of the nucleus.

- Non-relativistic description by solving the few-body Schrödinger equation:

$$(\hat{H}_0 + \hat{V})\,\Psi = E\,\Psi$$

- *Ab initio* calculations for the simplest cases (3B, 4B).
- Difficult problem due to the $N\bar{N}$ interaction, the annihilation dynamics, and the presence of different scales.

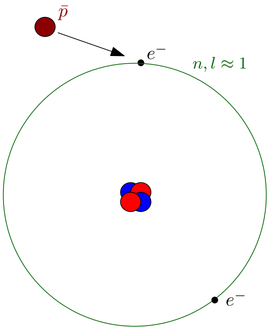

Figure: Antiproton-nucleus system

Antiproton-nucleus system

- Antiproton-nucleus system:
  1. Capture of the antiproton on a highly excited Coulomb orbital and formation of a quasi-bound state with

$$E = E_R - i\frac{\Gamma}{2}, \qquad E_R \approx E_B - \frac{\mathrm{Ryd}(\bar{\mathrm{p}}\mathrm{A})}{n^2}$$

  2. X-ray cascade and annihilation with a nucleon of the nucleus.

- Non-relativistic description by solving the few-body Schrödinger equation:

$$(\hat{H}_0 + \hat{V})\,\Psi = E\,\Psi$$

- *Ab initio* calculations for the simplest cases (3B, 4B).
- Difficult problem due to the $N\bar{N}$ interaction, the annihilation dynamics, and the presence of different scales.

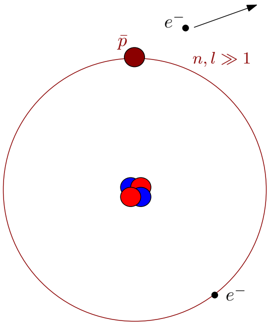

Figure: Antiproton-nucleus system

Antiproton-nucleus system

- Antiproton-nucleus system:
  1. Capture of the antiproton on a highly excited Coulomb orbital and formation of a quasi-bound state with

$$E = E_R - i\frac{\Gamma}{2}, \qquad E_R \approx E_B - \frac{\mathrm{Ryd}(\bar{\mathrm{p}}\mathrm{A})}{n^2}$$

  2. X-ray cascade and annihilation with a nucleon of the nucleus.

- Non-relativistic description by solving the few-body Schrödinger equation:

$$(\hat{H}_0 + \hat{V})\,\Psi = E\,\Psi$$

- *Ab initio* calculations for the simplest cases (3B, 4B).
- Difficult problem due to the $N\bar{N}$ interaction, the annihilation dynamics, and the presence of different scales.

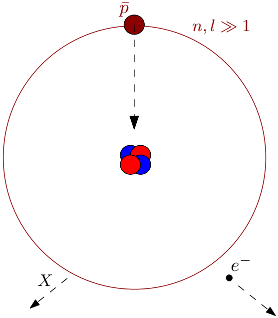

Figure: Antiproton-nucleus system

Outline

$N\bar{N}$ scattering

- Most of the $N\bar{N}$ scattering data come from the LEAR experiments.
- The $p\bar{p}$ scattering involves the elastic scattering ($p\bar{p} \to p\bar{p}$), the charge-exchange process ($p\bar{p} \to n\bar{n}$), and the annihilation ($p\bar{p} \to \pi\bar{\pi}, \pi\bar{\pi}\pi\bar{\pi}, \rho\bar{\rho}, ...$).

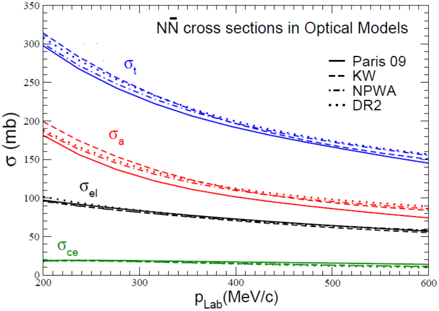

Figure: $N\bar{N}$ cross sections computed with different $N\bar{N}$ models[1]

[1] J. Carbonell, G. Hupin, and S. Wycech, *Eur. Phys. J. A* **59** (2023) 259

Protonium

- In the absence of strong nuclear interaction, $p\bar{p}$ would form an hydrogenic state with energy

$$\epsilon_n = -\frac{12.5}{n^2}\,\mathrm{keV}$$

  and with a Bohr radius $B_{p\bar{p}} = 57\,\mathrm{fm}$.
- The nuclear interaction shifts and broadens the energy levels.
  1. The level shift $\Delta E_n = \Delta E_r - i\frac{\Gamma}{2}$ has been measured for low lying states[1,2].
  2. The level shift is related to the scattering length.
- Privileged system to test the $N\bar{N}$ interaction at low-energy.
- Hard to extract useful information from the study of antiprotonic atoms to construct $N\bar{N}$ models.

[1] M. Augsburger *et al.*, *Nucl. Phys. A* **658** (1999) 149
[2] K. Heitlinger *et al.*, *Z. Phys. A* **342** (1992) 359

$N\bar{N}$ interaction from G-parity transform

- The meson exchange theory is the traditional way to formulate the NN interaction:

$$V_{NN} = V_{\sigma_0} + V_{\sigma_1} + V_\eta + V_\rho + V_\omega + V_\pi$$

- Old-fashioned, yet efficient.
- The associated $N\bar{N}$ interaction is obtained via G-parity transform, providing a factor $G = \pm 1$ for each meson:

$$V_{N\bar{N}} = V_{\sigma_0} - V_{\sigma_1} + V_\eta + V_\rho - V_\omega - V_\pi$$

- Repulsive parts become strongly attractive and tensor forces become huge $\longrightarrow$ deep bound and resonant states theoretically expected but never experimentally observed...
- **Real part only** $\longrightarrow$ Phenomenology required for the annihilation.
- More recent formulation using chiral effective field theory (Jülich[1]).

[1] L. Y. Dai, J. Haidenbauer, and U. G. Meißner. *J. High Energy Phys.* **1707** (2017) 78

$N\bar{N}$ annihilation

- The annihilation involves complex dynamics and many meson-producing channels, mainly pions[1]:

$$
\begin{aligned}
p\bar{p} &\to p\bar{p} \\
&\to n\bar{n} \\
&\to \pi^0\pi^0 \\
&\to \pi^0\pi^0\pi^0 \\
&\to \pi^0\pi^0\pi^0\pi^0 \\
&\to \pi^+\pi^- \\
&\to \pi^+\pi^-\pi^0 \\
&\to \pi^+\pi^-\pi^0\pi^0 \\
&\to \pi^+\pi^-\pi^+\pi^- \\
&\ \ \vdots
\end{aligned}
\qquad\qquad
\begin{aligned}
n\bar{p} &\to n\bar{p} \\
&\to \pi^-\pi^0 \\
&\to \pi^-\pi^0 \\
&\to \pi^-\pi^-\pi^+ \\
&\to \pi^-\pi^-\pi^+\pi^0 \\
&\to \pi^-\pi^-\pi^+\pi^0 \\
&\to \pi^-\pi^-\pi^-\pi^+\pi^+ \\
&\to \pi^-\pi^-\pi^-\pi^+\pi^+\pi^0 \\
&\to \pi^-\pi^-\pi^-\pi^-\pi^+\pi^+\pi^+\pi^0 \\
&\ \ \vdots
\end{aligned}
$$

- The $N\bar{N}$ channels are treated explicitly.
- The meson channels are treated by using phenomenological models.

[1] T. Aumann, A. Obertelli, *et al.* *Eur. J. Phys. A* **58** (2022) 88

Optical model

- The annihilation is traditionally treated with optical potentials:

$$V_{N\bar{N}} \to V_{N\bar{N}} + W_R + iW_I$$

- The imaginary part W_I induces a loss of probability current in the initial channel which simulates the effect of all annihilation channels.
- The form of $W = W_R + iW_I$ is usually a Woods-Saxon well[1] : $W(r) = \frac{-W_0}{1+\exp\left[\frac{r-R}{a}\right]}$.

	Dover-Richard 1	Dover-Richard 2	Kohno-Weise
W_0 (GeV)	$21 + 20\,\mathrm{i}$	$0.5 + 0.5\,\mathrm{i}$	$1.2\,\mathrm{i}$
R (fm)	0.0	0.80	0.55
a (fm)	0.2	0.2	0.2

- Quite successful despite its simplicity.
- Non-unitary S matrix: a part of the flux goes nowhere $\longrightarrow |S^\dagger S| < 1$.

[1] C. B. Dover, T. Gutsche, M. Maruyama, and A. Faessler. *Prog. Part. Nucl. Phys.* **29** (1992) 87

Optical model: protonium

- All models roughly reproduce low-energy observables and integrated cross sections.
- Reasonable agreement with experimental data.

	$^1S_0$ (keV)		$^3SD_1$ (keV)	
	ΔE_r	$\Gamma/2$	ΔE_r	$\Gamma/2$
DR1	0.54	0.51	0.77	0.45
DR2	0.58	0.52	0.82	0.46
KW	0.50	0.63	0.78	0.49
Paris 09	0.81	0.55	0.70	0.40
Jülich	0.44	0.59	0.78	0.64
Exp.	$0.44_{\pm 0.08}$	$0.60_{\pm 0.13}$	$0.78_{\pm 0.04}$	$0.47_{\pm 0.04}$

Table: Level shifts for S waves (keV).

- But, "large and systematic differences have been observed in almost all the partial waves"[1].

[1] J. Carbonell, G. Hupin, and S. Wycech, *Eur. Phys. J. A* **59** (2023) 259

Optical model: protonium

- All models roughly reproduce low-energy observables and integrated cross sections.
- Reasonable agreement with experimental data.

	$^3P_0$ (meV)		$^1P_1$ (meV)	
	ΔE_r	$\Gamma/2$	ΔE_r	$\Gamma/2$
DR1	-74	57	-26	13
DR2	-62	40	-24	14
KW	-69	48	-29	13
Paris 09	-65	53	-29	14
Jülich	-16	84		
Exp.	$-139_{\pm 28}$	$60_{\pm 13}$		

Table: Level shifts for P waves (meV).

- But, "large and systematic differences have been observed in almost all the partial waves"[1].

[1] J. Carbonell, G. Hupin, and S. Wycech, *Eur. Phys. J. A* **59** (2023) 259

Coupled-channel model

- The annihilation is simulated by the addition of effective meson-antimeson ($m\bar{m}$) channels mimicking the real ones.
- Still phenomenological but provides a more realistic description of the annihilation process and involves quite different dynamics ($S^\dagger S = \mathbb{I}$).
- To investigate the model dependence, the parameters of the coupled-channel potential are here adjusted to fit the optical model results.

  - Annihilation channels:

$$\begin{aligned} p\bar{p} &\to p\bar{p} \\ &\to m_1\bar{m}_1 \\ &\to n\bar{n} \\ &\to m_2\bar{m}_2 \end{aligned}$$

$$\begin{aligned} n\bar{p} &\to n\bar{p} \\ &\to m_3\bar{m}_3 \end{aligned}$$

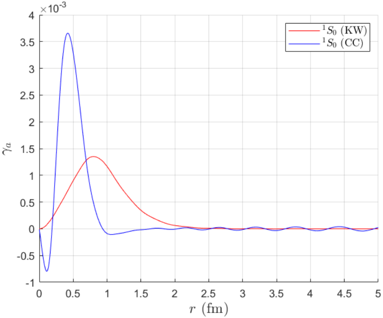

Figure: $p\bar{p}$ annihilation densities ($^1S_0$)

Outline

Faddeev equations (3-body systems)

- Decomposition of the wavefunction in Faddeev components[1]: $\Psi = \Psi_1 + \Psi_2 + \Psi_3$
- The Faddeev components are solutions of

$$(E - H_0 - V_i)\Psi_i(\boldsymbol{x}_i, \boldsymbol{y}_i) = V_i\left[\Psi_j(\boldsymbol{x}_j, \boldsymbol{y}_j) + \Psi_k(\boldsymbol{x}_k, \boldsymbol{y}_k)\right], \quad (ijk) = (123), (312), (231)$$

- Independent boundary condition for each Faddeev component $\longrightarrow$ adapted for scattering problems.
- However, corrections required for long-range potentials.

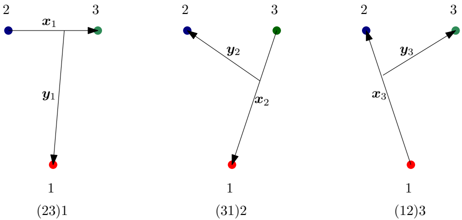

Figure: Jacobi coordinates for a three-body system

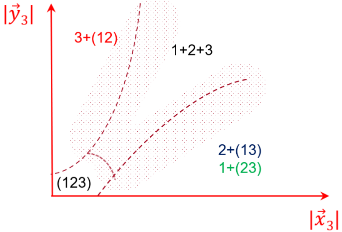

Figure: Partitions of the system

[1] L. D. Faddeev. *Sov. Phys. JETP* **39** (1960) 1459

Faddeev-Merkuriev equations

- To ensure the asymptotic decoupling of the Faddeev components, the Coulomb potential is separated into a short-range and a long-range part:

$$V_i = V_i^{(s)} + V_i^{(l)}$$

- The Faddeev equations become[1]

$$(E - H_0 - V_i - \sum_{j \neq i} V_j^{(l)})\Psi_i(\boldsymbol{x}_i, \boldsymbol{y}_i) = V_i^{(s)} \left[\Psi_j(\boldsymbol{x}_j, \boldsymbol{y}_j) + \Psi_k(\boldsymbol{x}_k, \boldsymbol{y}_k)\right]$$

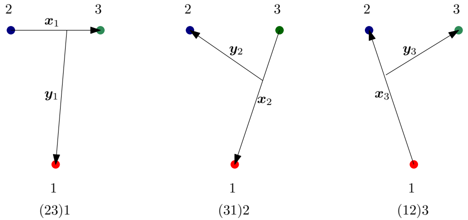

Figure: Jacobi coordinates for a three-body system

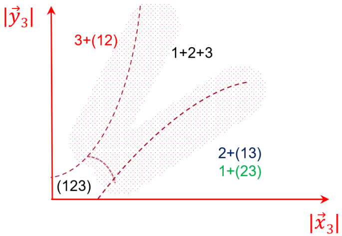

Figure: Partitions of the system

[1] S. P. Merkuriev. *Ann. Phys.* **130** (1980) 395

Partial wave expansion

- Resolution with a partial wave expansion:

$$\Psi_i(\boldsymbol{x}_i, \boldsymbol{y}_i) = \sum_{n=l_x,l_y,L,s_x,S,t_x,T} \frac{\phi_n^{(i)}(x_i, y_i)}{x_i y_i} \left\{ [l_x l_y]_L \left[(s_j s_k)_{s_x} s_i \right]_S \right\}_J$$

- The radial functions are expressed as a linear combination of Lagrange functions:

$$\phi_n^{(i)}(x_i, y_i) = \sum_{\alpha,\beta} c_{n\alpha\beta}^{(i)} \hat{f}_\alpha \left(\frac{x_i}{h_x^{(i)}} \right) \hat{f}_\beta \left(\frac{y_i}{h_y^{(i)}} \right)$$

- Lagrange function: polynomial multiplied by an exponential function, behaving as r^{l+1} close to the origin.
- Resolution of an eigenvalue problem for bound states.
- Resolution of linear systems for scattering states.
- Matrices of large dimension $\longrightarrow$ iterative methods (Power method, Lanczos algorithm, GMRES, BICGSTAB,...).

Deuteron-antiproton system: optical model

- Additional Faddeev components to account for the charge-exchange process $\longrightarrow$ 6 FM components[1]
- Symmetry of the wavefunction $\longrightarrow$ 5 FM equations

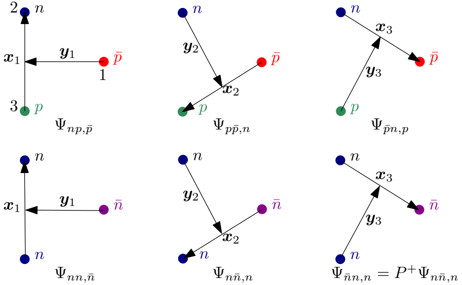

Figure: Faddeev components for the $d\bar{p}$ system (optical model)

[1] R. Lazauskas, and J. Carbonell, *Phys. Lett. B* **820** (2021) 136573

Deuteron-antiproton system: coupled-channel model

- Additional Faddeev components to account for the coupling with other particle channels $\longrightarrow$ 15 FM components
- Symmetry of the wavefunction + non-interacting mesons $\longrightarrow$ 8 FM equations

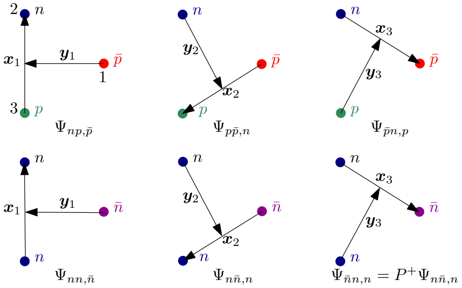

Figure: Faddeev components for the $d\bar{p}$ system (coupled-channel model)

Deuteron-antiproton system: coupled-channel model

- Additional Faddeev components to account for the coupling with other particle channels $\longrightarrow$ 15 FM components
- Symmetry of the wavefunction + non-interacting mesons $\longrightarrow$ 8 FM equations

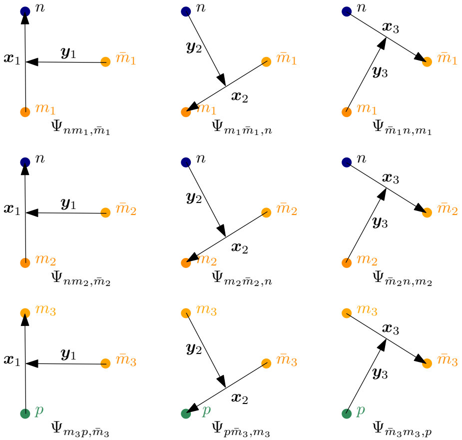

Figure: Faddeev components for the $d\bar{p}$ system (coupled-channel model)

Outline

Scattering length

- Study of the zero-energy $d\bar{p}$ collision $\longrightarrow$ scattering length a_l.
- Complex scaling to handle the three-body breakup in meson channels.

	MT+KW[1]	MT+CC[2]	AV18+KW[1]	AV18+CC[2]
	a_0 (fm)	a_0 (fm)	a_0 (fm)	a_0 (fm)
$S^+_{1/2}$	$1.34 - 0.72\,\mathrm{i}$	$1.32 - 0.71\,\mathrm{i}$	$1.34 - 0.72\,\mathrm{i}$	$1.31 - 0.68\,\mathrm{i}$
$S^+_{3/2}$	$1.39 - 0.72\,\mathrm{i}$	$1.40 - 0.73\,\mathrm{i}$	$1.39 - 0.72\,\mathrm{i}$	$1.39 - 0.74\,\mathrm{i}$
	a_1 (fm^3)	a_1 (fm^3)	a_1 (fm^3)	a_1 (fm^3)
$P^-_{5/2}$	$0.71 - 2.64\,\mathrm{i}$	$0.68 - 2.73\,\mathrm{i}$	$0.70 - 2.60\,\mathrm{i}$	$0.64 - 2.59\,\mathrm{i}$

- Small dependence on the NN and on the $\bar{N}N$ interactions.
- Quite good agreement between the KW and CC models within few percent despite their very different dynamics.

[1] P.-Y. Duerinck, R. Lazauskas, and J. Carbonell, *Phys. Lett. B* **841** (2023) 137936 (corrigendum)

[2] P.-Y. Duerinck, R. Lazauskas, and J. Dohet-Eraly, *Phys. Rev. C* **108** (2023) 054003

Energy shift and Trueman relation

- In the absence of strong nuclear interaction between the deuteron and the antiproton would form an hydrogenic state with energy

$$E = -2.22\ \text{MeV} + \epsilon_n, \quad \epsilon_n = -\frac{16.7}{n^2}\ \text{keV}$$

- The nuclear interaction shifts and broadens the energy levels:

$$E = -2.22\ \text{MeV} + E_n - i\frac{\Gamma}{2}$$

- The energy can be calculated by computing the eigenvalues of the Hamiltonian (optical model) and of the complex-scaled Hamiltonian (coupled-channel model).
- Alternative approach: computing the energy shift from the scattering length by using the Trueman relation[1]. For S waves, it reads

$$\Delta E_n = E_n - i\frac{\Gamma}{2} - \epsilon_n = -\frac{4}{n}\,\frac{a_0}{B_{d\bar{p}}}\,\epsilon_n$$

[1] T. L. Trueman, *Nucl. Phys.* **26** (1961) 57

Energy shift and Trueman relation

- Trueman relation: consistent results with the calculation of the eigenvalues.
- Easier way to compute the energy shifts.

	MT+KW[1]		MT+CC[2]	
	ΔE_n (keV)	$\Delta E_n^{(\mathrm{T})}$ (keV)	ΔE_n (keV)	$\Delta E_n^{(\mathrm{T})}$ (keV)
$S_{1/2}^{+}$	$1.92 - 0.89\,\mathrm{i}$	$1.92 - 0.89\,\mathrm{i}$	$1.91 - 0.86\,\mathrm{i}$	$1.90 - 0.88\,\mathrm{i}$
$S_{3/2}^{+}$	$2.00 - 0.89\,\mathrm{i}$	$1.99 - 0.88\,\mathrm{i}$	$1.98 - 0.90\,\mathrm{i}$	$1.99 - 0.90\,\mathrm{i}$
	ΔE_n (meV)	$\Delta E_n^{(\mathrm{T})}$ (meV)	ΔE_n (meV)	$\Delta E_n^{(\mathrm{T})}$ (meV)
$P_{5/2}^{-}$	$51.8 - 213\,\mathrm{i}$	$55.4 - 205\,\mathrm{i}$	/	$52.8 - 212\,\mathrm{i}$
	AV18+KW[1]		AV18+CC[2]	
	ΔE_n (keV)	$\Delta E_n^{(\mathrm{T})}$ (keV)	ΔE_n (keV)	$\Delta E_n^{(\mathrm{T})}$ (keV)
$S_{1/2}^{+}$	$1.91 - 0.89\,\mathrm{i}$	$1.92 - 0.89\,\mathrm{i}$	$1.87 - 0.86\,\mathrm{i}$	$1.88 - 0.85$
$S_{3/2}^{+}$	$1.99 - 0.89\,\mathrm{i}$	$1.98 - 0.89\,\mathrm{i}$	$1.84 - 0.95\,\mathrm{i}$	$1.98 - 0.91\,\mathrm{i}$
	ΔE_n (meV)	$\Delta E_n^{(\mathrm{T})}$ (meV)	ΔE_n (meV)	$\Delta E_n^{(\mathrm{T})}$ (meV)
$P_{5/2}^{-}$	$61.2 - 207\,\mathrm{i}$	$54.2 - 202\,\mathrm{i}$	/	$49.9 - 201\,\mathrm{i}$

[1] P.-Y. Duerinck, R. Lazauskas, and J. Carbonell, *Phys. Lett. B* **841** (2023) 137936 (corrigendum)

[2] P.-Y. Duerinck, R. Lazauskas, and J. Dohet-Eraly, *Phys. Rev. C* **108** (2023) 054003

Comparison with other optical potentials

- Low dependence on both NN and $N\bar{N}$ interactions for S waves.
- Larger dispersion, yet comparable results for the $P^-_{5/2}$ state.

$S^+_{1/2}(n=1)$ (keV)	DR1	DR2	KW	Jülich
MT-I-III	$1.98 - 0.75$i	$2.02 - 0.74$i	$1.93 - 0.91$i	
AV18	$1.97 - 0.74$i	$2.01 - 0.74$i	$1.92 - 0.90$i	
I-N3LO			$1.92 - 0.89$i	$1.84 - 0.89$i
$S^+_{3/2}(n=1)$ (keV)	DR1	DR2	KW	Jülich
MT-I-III	$2.02 - 0.75$i	$2.06 - 0.76$i	$1.98 - 0.91$i	
AV18	$2.03 - 0.73$i	$2.08 - 0.75$i	$1.97 - 0.91$i	
I-N3LO			$1.99 - 0.89$i	$1.97 - 1.14$i
$P^-_{5/2}(n=2)$ (meV)	DR1	DR2	KW	Jülich
MT-I-III	$92.9 - 192$i	$95.1 - 209$i	$52.4 - 208$i	
AV18	$91.5 - 185$i	$93.6 - 193$i	$51.7 - 201$i	
I-N3LO				$33.1 - 219$i

Table: Level shifts for S (keV) and P waves (meV) computed with different $NN + N\bar{N}$ interactions.

Comparison with experiment

- Our results are the exact solution (in the numerical sense) of the three-body problem.
- Strong discrepancy with experimental data, especially for ΔE_R ($\sim 4\sigma$).

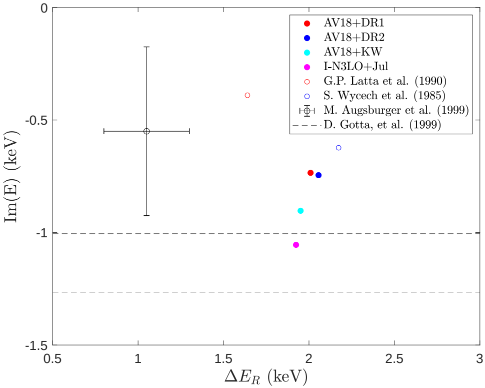

Figure: Comparison of the spin-average S wave level shifts and widths with previous results and experiments.

The case of coupled waves

- The Trueman relation works well for uncoupled waves but is not valid for spin-coupled ones such as $P^{-}_{1/2}$, $P^{-}_{3/2}$ due to long-range terms in $\frac{1}{r^3}$ arising from the quadrupole moment of the deuteron.
- Strong differences are therefore observed when comparing results obtained with central and realistic NN interactions.

	MT+KW	AV18+KW
$^2P_{1/2}(n=2)$	$45.3 - 194.1$i	$-28.4 - 226.6$i
$^4P_{1/2}(n=2)$	$69.0 - 243$i	$213.0 - 184.9$i
$^2P_{1/2}(n=3)$	$15.9 - 68.1$i	$-4.7 - 79.4$i
$^4P_{1/2}(n=3)$	$24.2 - 85.3$i	$63.2 - 65.1$i

Table: $P^{-}_{1/2}$ level shifts (meV) computed with different NN interactions.

$N\bar{N}$ model-dependence

- While a nice agreement is observed for S waves, sizeable differences are found in some P waves, which is also observed in protonium.

	I-N3LO+KW	I-N3LO+Jülich
${}^2P_{1/2}(n=2)$	$-25.9 - 229$i	$38.7 - 268$i
${}^4P_{1/2}(n=2)$	$218 - 190$i	$192 - 220$i
${}^2P_{1/2}(n=3)$	$-3.6 - 80.1$i	$25.7 - 95.9$i
${}^4P_{1/2}(n=3)$	$60.7 - 46.0$i	$48.8 - 75.4$i
${}^2P_{3/2}(n=2)$	$58.2 - 193$i	$54.0 - 163$i
${}^4P_{3/2}(n=2)$	$-38.9 - 228$i	$-83.6 - 215$i
${}^2P_{3/2}(n=3)$	$18.8 - 67.7$i	$17.5 - 57.1$i
${}^4P_{3/2}(n=3)$	$-8.4 - 80.0$i	$-24.2 - 75.4$i

Table: Coupled P waves level shifts (meV) computed with different $N\bar{N}$ interactions.

Annihilation density

- The annihilation density $\gamma_a(r)$ is related to the probability of annihilation of the antiproton in space:

$$\Gamma = \int \gamma_a(r)\mathrm{d}r$$

- For the P wave, the annihilation density scales with the deuteron density $\longrightarrow$ peripheral absorption.
- For the S wave, the annihilation is less peripheral.

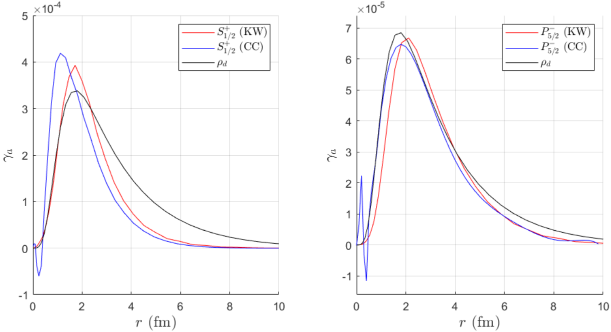

Figure: Annihilation density for S wave (left) and P wave (right).

Outline

Conclusion

- Investigation of the model-dependence in the $d\bar{p}$ system by comparing different $N\bar{N}$ models (optical, coupled-channel).
- $d\bar{p}$ level shifts:
  1. Low dependence on both NN and $N\bar{N}$ interactions for S waves.
  2. Strong model-dependence in some P waves $\longrightarrow$ our understanding of the $N\bar{N}$ interaction can be improved.
  3. Despite their very different dynamics, the optical and coupled-channel models provide quite similar results $\longrightarrow$ highlights the interest for optical models given their relative simplicity.
  4. Trueman relation valid to compute the level shift of uncoupled states.
- Annihilation densities: the annihilation is expected to be peripheral, at least for P waves $\longrightarrow$ supports the major hypothesis of PUMA experiments.
- Prospects:
  1. Study of $\frac{1}{r^3}$ terms in $p\bar{p}$ and $d\bar{p}$ systems (magnetic, quadrupole).
  2. Extension of the formalism to four-body systems (Faddeev-Yakubovsky): $^3\mathrm{H} + \bar{\mathrm{p}}$, $^3\mathrm{He} + \bar{\mathrm{p}}$.